Pediatr Radiol (2016) 46:983–990
DOI 10.1007/s00247-016-3553-7

ORIGINAL ARTICLE

Free-breathing motion-corrected late-gadolinium-enhancement imaging improves image quality in children

Laura Olivieri[1,2] · Russell Cross[1] · Kendall J. O'Brien[1,2] · Hui Xue[2] · Peter Kellman[2] · Michael S. Hansen[2]

Received: 26 September 2015 / Revised: 16 December 2015 / Accepted: 21 January 2016 / Published online: 17 February 2016

Abstract
Background The value of late-gadolinium-enhancement (LGE) imaging in the diagnosis and management of pediatric and congenital heart disease is clear; however current acquisition techniques are susceptible to error and artifacts when performed in children because of children's higher heart rates, higher prevalence of sinus arrhythmia, and inability to breath-hold. Commonly used techniques in pediatric LGE imaging include breath-held segmented FLASH (segFLASH) and steady-state free precession-based (segSSFP) imaging. More recently, single-shot SSFP techniques with respiratory motion-corrected averaging have emerged.
Objective This study tested and compared single-shot free-breathing LGE techniques with standard segmented breath-held techniques in children undergoing LGE imaging.
Materials and methods Thirty-two consecutive children underwent clinically indicated late-enhancement imaging using intravenous gadobutrol 0.15 mmol/kg. Breath-held segSSFP, breath-held segFLASH, and free-breathing single-shot SSFP LGE sequences were performed in consecutive series in each child. Two blinded reviewers evaluated the quality of the images and rated them on a scale of 1–5 (1 = poor, 5 = superior) based on blood pool–myocardial definition, presence of cardiac motion, presence of respiratory motion artifacts, and image acquisition artifact. We used analysis of variance (ANOVA) to compare groups.
Results Patients ranged in age from 9 months to 18 years, with a mean +/− standard deviation (SD) of 13.3 +/− 4.8 years. R-R interval at the time of acquisition ranged 366–1,265 milliseconds (ms) (47–164 beats per minute [bpm]), mean +/− SD of 843+/−231 ms (72+/−21 bpm). Mean +/− SD quality ratings for long-axis imaging for segFLASH, segSSFP and single-shot SSFP were 3.1+/−0.9, 3.4+/−0.9 and 4.0+/−0.9, respectively ($P<0.01$ by ANOVA). Mean +/− SD quality ratings for short-axis imaging for segFLASH, segSSFP and single-shot SSFP were 3.4+/−1, 3.8+/−0.9 and 4.3+/−0.7, respectively ($P<0.01$ by ANOVA).
Conclusion Single-shot late-enhancement imaging with motion-corrected averaging is feasible in children, robust at high heart rates and with variable R-R intervals, and can be performed without breath-holding with higher image quality ratings than standard breath-held techniques. Use of free-breathing single-shot motion-corrected technique does not compromise LGE image quality in children who can hold their breath, and it can significantly improve image quality in children who cannot hold their breath or who have significant arrhythmia.

Keywords Children · Free breathing · Heart · Late gadolinium enhancement · Magnetic resonance imaging

✉ Laura Olivieri
lolivier@childrensnational.org

[1] Division of Cardiology, Children's National Health System, W3-200, 111 Michigan Ave. NW, Washington, DC 20010, USA

[2] National Heart, Lung and Blood Institute, National Institutes of Health, Bethesda, MD, USA

Introduction

The value of late-gadolinium-enhancement (LGE) imaging in the diagnosis and management of pediatric and congenital heart disease has been documented in the literature for over a decade. The impact of late-gadolinium-enhancement findings in congenital heart disease [1, 2], pediatric muscular dystrophies [3] and pediatric hypertrophic cardiomyopathy [4] are significant and widely published. Additionally, LGE imaging has been performed in children and adults with myocarditis [5], anthracycline exposure [6] and myocardial infarction, with important clinical implications already established in the literature. LGE imaging is typically performed using a T1-weighted inversion recovery sequence with either a segmented steady-state free precession readout or a segmented FLASH (gradient-recalled-echo-based) readout. Both have T1 weighting because of the inversion recovery preparation that allows for nulling of normal myocardium and elevated signal intensity in regions of cardiac muscle where gadolinium has collected. The segmented FLASH has been reported to have slightly better contrast-to-noise ratio when compared to SSFP [7]. Traditionally a segmented breath-held approach is used to produce LGE images, where inversion times are typically 250–350 ms, requiring 8–14 heartbeats to acquire data to produce one image. Although the utility of LGE is clear, current techniques are susceptible to error and artifacts when performed in children because of children's higher heart rates and higher prevalence of sinus arrhythmia, and the use of lower slice thickness leading to lower signal-to-noise ratio. Additionally, it can be difficult for children to comply with breath-holding instructions for reasons related to their development or their cardiovascular disease state. Finally, a significant portion of pediatric studies is performed with sedation, where breath-holding would require general anesthesia and mechanical breath-holding, imparting a longer recovery and introducing more risk to the imaging procedure [8].

The use of a single-shot SSFP-based technique has been described in adults and has been found to detect infarction and fibrosis [9, 10]. The use of respiratory-motion-corrected averaging in conjunction with repeated single-shot SSFP LGE improves the signal-to-noise ratio, thereby permitting the use of improved spatial and temporal resolution [11–13]. Its utility as an imaging biomarker for long-term outcomes in adults with cardiac disease has been described [14]. Although the single-shot imaging with acceleration factor 2 has a lower signal-to-noise ratio when compared to the segmented methods, signal can be regained through image averaging over multiple cardiac cycles. Both approaches (segmented breath-held, and single-shot free-breathing) have similar acquisition times. Thus our hypothesis was that equivalent image quality can be obtained with single-shot imaging, and that superior image quality can be obtained in the presence of arrhythmia and inability to breath-hold.

Therefore this study tested and compared single-shot free-breathing LGE techniques with standard segmented breath-held techniques in children and young adults undergoing LGE imaging.

Materials and methods

Our institutional review board approved this study, and we obtained written informed consent from all 32 consecutive participants. Gadobutrol 0.15 mmol/kg (Bayer Healthcare, Whippany, NJ) was administered intravenously for clinical indications, including evaluation for myocarditis or cardiomyopathy, or for thoracic arterial and venous anatomy requiring an angiogram, after which research LGE images were obtained. Late-gadolinium-enhancement imaging was performed on a Siemens 1.5-T Aera (Siemens Healthcare, Erlangen, Germany) 10–15 min after the infusion. Inversion time was selected from a modified Look-Locker sequence based on the inversion time where myocardium was best nulled. For clinical purposes, a standard series of LGE imaging was performed in patients in whom respiration could be suspended, either by request/direction or by suspending respiration in an anesthetized child. Inversion time was adjusted, and an additional segmented FLASH (segFLASH), segmented SSFP (segSSFP) and free-breathing motion-corrected single-shot SSFP image were taken in short-axis and long-axis orientations according to the left ventricle in each patient in consecutive series, for a total of six images. Short-axis image position was at the mid-ventricular level or at the level of LGE, if present. The order of these six images was randomized. All six images were completed within 2 min, and within 15 min of gadolinium administration. Breath-hold times for segFLASH and segSSFP were comparable — generally within 1–3 s, depending on R-R interval during acquisition, and no standard arrhythmia rejection was used. The respiratory-motion-corrected reconstructions took 10–15 s.

Imaging parameters for segmented FLASH, segmented SSFP and single-shot SSFP for children weighing less than 15 kg and for those weighing more than 15 kg are described in Tables 1 and 2, respectively. All patients were imaged with one of these sets of parameters in order to standardize the imaging experiment. We used standard imaging parameters for the breath-held segmented LGE sequences to maintain a uniform and optimized image resolution. Imaging was generally completed over 70–100 ms per R-R interval for small patients and over 140–200 ms for larger patients. A standard trigger delay of 150–250 ms was added, based on the R-R interval, to situate the readout window in mid-diastole. For single-shot SSFP, eight repetitions were acquired and four measurements were averaged with online reconstruction after motion correcting; four measurements were discarded to mitigate through-plane motion.

Motion correction was performed using non-rigid registration of the single-shot images to a common target frame. The common target frame was selected as the frame that was similar to most other frames with regard to root mean square difference. The four frames that were the most similar frames prior to registration were averaged after non-rigid registration,

Table 1 Imaging parameters for late-gadolinium-enhancement (LGE) imaging for segmented FLASH (segFLASH), segmented steady-state free precession (segSSFP) and single-shot SSFP (ssSSFP) for children weighing less than 15 kg

Imaging parameter	segFLASH	segSSFP	ssSSFP
FOV	228 × 171	228 × 171	228 × 171
Slice thickness	6 mm	6 mm	6 mm
Matrix size	128 × 78	128 × 81	128 × 82
Flip angle	25	50	50
TE	3.19 ms	1.1 ms	1.2 ms
TR	8.11 ms	2.62 ms	2.53 ms
Shots per slice	6	3	1
Views per segment	13	27	41
Acquisition window	105 ms	71 ms	103 ms
R-R interval	Every 4th	Every 4th	Every 4th
Acceleration	1	1	2
Averages	1	1	4 of 8

FLASH fast low angle shot, *FOV* field of view, *TE* echo time, *TR* repetition time

and the four frames that were the most different from other frames were discarded to avoid problems with through-plane motion [12]. The non-rigid registration algorithm produces pixel-wise deformation fields, which are needed to warp the single-shot LGE images before the averaging. To estimate the deformation field, a fast variational image registration framework is applied as the working engine [15]. This approach can be considered as an extension of the classic optical flow method. In this framework, a dense pixel-wise deformation field is estimated as the solution to a calculus of variation problem, which is solved by performing a compositional update step corresponding to a partial differential transport equation. Regularization is added by low-pass filtering of the gradient images, which are in turn used as a velocity field to drive the transport equation. To speed up the convergence and avoid local minima, a multi-scale image pyramid is created. The local cross correlation [16] was selected as the image similarity measure because its explicit derivative can be efficiently calculated while being general enough to cope with noise and intensity differences among single-shot LGE images. After computing the deformation fields, we warped the single-shot images using a fifth-order BSpline interpolator and used them for averaging.

Table 2 Imaging parameters for late-gadolinium-enhancement (LGE) imaging for segmented FLASH (segFLASH), segmented steady-state free precession (segSSFP) and single-shot SSFP (ssSSFP) for patients weighing more than 15 kg

Imaging parameter	segFLASH	segSSFP	ssSSFP
FOV	332 × 249	332 × 249	332 × 249
Slice thickness	8 mm	8 mm	8 mm
Matrix size	256 × 144	256 × 144	256 × 144
Flip angle	25	50	50
TE	3.2 ms	1.23 ms	1.23 ms
TR	8.31 ms	2.91 ms	2.91 ms
Shots per slice	6	3	1
Views per segment	24	48	72
Acquisition window	199 ms	140 ms	209 ms
R-R interval	Every 2nd	Every 2nd	Every 4th
Acceleration	1	1	2
Averages	1	1	4 of 8

FLASH fast low angle shot, *FOV* field of view, *TE* echo time, *TR* repetition time

Of note, and central to this study, patients who were scanned without sedation were asked to give a best effort to comply with breath-holding techniques. Patients who were scanned using general anesthesia had respirations suspended for the breath-held techniques. Patients who were scanned while free-breathing with sedation (without the ability to suspend respiration, either by command or with general anesthesia), were not included in this study because of the inability to compare a breath-held image with a non-breath-held image in the same patient. It is standard at our institution to use sedation and anesthesia only if absolutely clinically indicated.

Phase-sensitive images were first randomized and assigned quality scores by two blinded and independent reviewers. Quality scores were assigned based on the degree of cardiorespiratory motion, ranging from 1 (poor) to 5 (superior) as demonstrated in Fig. 1. Specifically, quality was assigned 1, or poor, when one could only identify blood pool and myocardium; 2, or fair, when there were significant cardiorespiratory motion artifacts and blood pool–myocardial border blurring; 3, or satisfactory, when there were minimal cardiorespiratory artifacts and some blood pool–myocardial border blurring; 4, or good, when there were minimal cardiorespiratory artifacts and good blood pool–myocardial border distinction; and 5, or superior, when there were no cardiorespiratory artifacts or myocardial border blurring and images showed an easily discernable pericardium, myocardium and blood pool. Artifacts related to metal objects or poorly selected inversion time should be equal between the imaging groups and therefore were not taken into account in the overall quality rating.

The image quality key guided the image review and quality rating. Quality scores for the cohort were tallied and compared between the segmented FLASH (segFLASH), segmented SSFP (segSSFP) and single-shot SSFP (ssSSFP) using ANOVA with post-hoc analysis using the Student-Newman-Keuls test. The effect of heart rate on image-quality score was examined through calculation of a standard R^2 correlation coefficient. Additionally, a subgroup of patients with high-quality (>3) segmented images was identified to offer comparison between the methods, while excluding poor

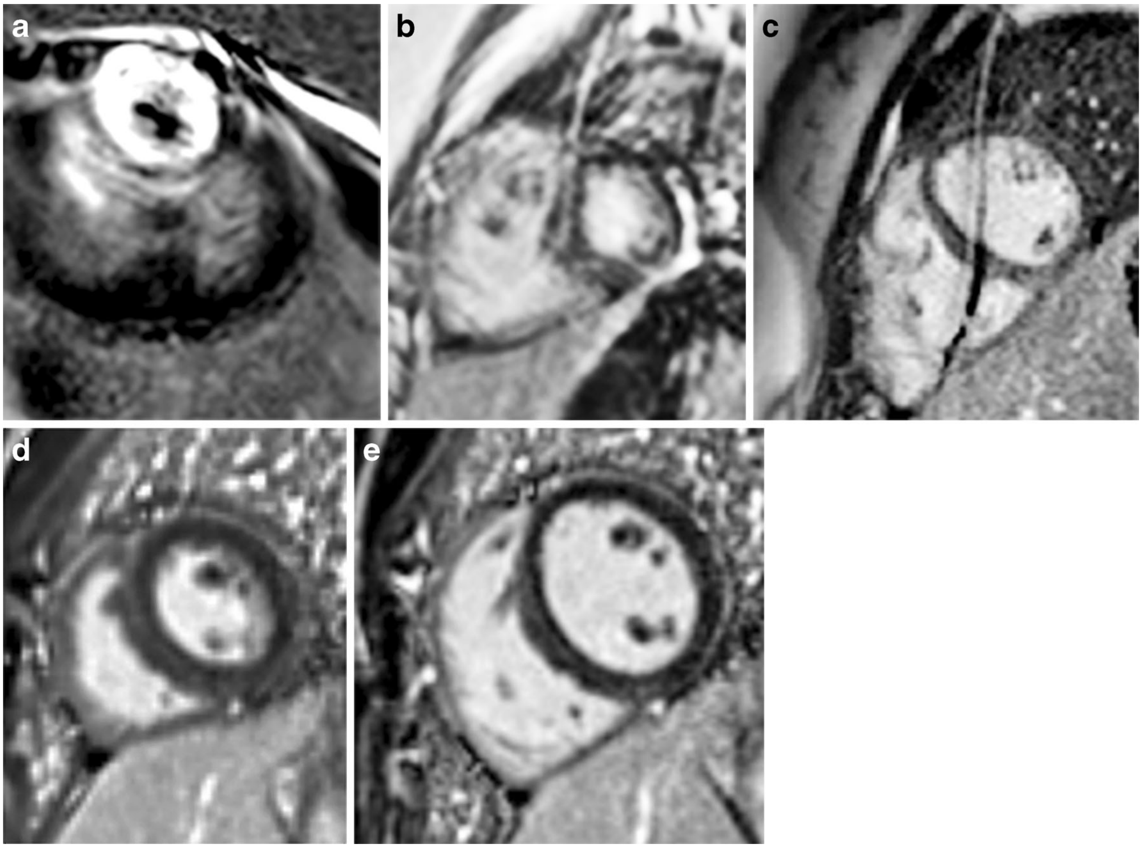

Fig. 1 Image quality key demonstrates images that are representative of each quality score, 1–5. **a** Quality score of 1, or poor. Can only identify blood pool and myocardium. **b** Image quality of 2, or fair. Significant cardiorespiratory motion artifacts and blood pool–myocardial border blurring. **c** Image quality of 3, or satisfactory. Minimal cardiorespiratory artifacts, some blood pool–myocardial border blurring. **d** Image quality of 4, or good. Minimal cardiorespiratory artifacts, good blood pool–myocardial border distinction. **e** Image quality of 5, or superior. No cardiorespiratory artifacts and no myocardial border blurring, with easily discernable pericardium, myocardium and blood pool

segmented images, and was compared using ANOVA. Finally, a group of patients with significant arrhythmias was identified by a pediatric cardiologist through review of all vectocardiogram tracings during image acquisition, and the segmented and free-breathing quality scores were compared using ANOVA.

Results

We included 32 children and young adults who ranged in age from 9 months to 18 years, with mean +/− SD of 13.3+/−4.8 years. R-R interval at the time of acquisition ranged 366–1,265 ms (47–164 bpm), mean +/− SD of 843+/−231 ms (72+/−21 bpm). Overall during LGE imaging, three patients had isolated premature ventricular contractions, one had isolated premature atrial contractions and six had sinus arrhythmia causing significant R-R interval variation. Table 3 illustrates the baseline characteristics of the group. For the entire cohort, mean +/− SD quality ratings for long-axis imaging for segmented breath-held FLASH (segFLASH), segmented SSFP (segSSFP) and single-shot SSFP (ssSSFP) were 3.1+/−0.9, 3.4+/−0.9 and 4.0+/−0.9, respectively ($P<0.01$ by ANOVA). Mean +/− SD quality ratings for short-axis imaging for segFLASH, segSSFP and ssSSFP were 3.4+/−1, 3.8+/−0.9 and 4.3+/−0.7, respectively ($P<0.01$ by ANOVA). Using a Student-Newman-Keuls test for all pairwise comparisons in a post-hoc analysis, the single-shot

Table 3 Baseline characteristics of the pediatric cohort undergoing late-enhancement imaging ($n=32$)

	Mean	SD	Min	Max
Age (y)	13.3	4.8	0.75	18
Height (cm)	151	29.4	58	188
Weight (kg)	59	25.8	5	120.6
BSA (m^2)	1.55	0.5	0.28	2.51
R-R interval (ms)	843	214	366	1265

BSA body surface area, *Max* maximum, *Min* minimum, *SD* standard deviation, *y* years

SSFP image-quality scores were different from both of the segmented image-quality scores. Finally, the kappa statistic ranged from 0.59 to 0.64 for each type of imaging, and there were no statistically significant differences between reviewers' aggregate scores for each type of imaging.

Effect of segmented imaging quality on single-shot SSFP score

We eliminated 16 patients who had segmented late enhancement images with a quality score less than 3 and performed a subgroup analysis to compare good-quality segmented images and corresponding ssSSFP images. Notably, the 16 excluded patients included all patients with arrhythmias, and these patients tended to be younger and smaller and have higher heart rates. A comparison of the remaining 16 patients' quality scores showed quality ratings of 3.6, 3.8 and 4.4 for segFLASH, segSSFP and ssSSFP in the long-axis projection, and 4, 4.3 and 4.6 for segFLASH, segSSFP and ssSSFP in the short-axis projection ($P<0.001$). Therefore, even in good-quality segmented imaging, the motion-corrected free-breathing late-enhancement sequence had higher quality ratings than the traditional segmented approach. Figure 2 demonstrates such a patient, where all three methods yield excellent-quality imaging.

Although quality ratings were significantly and universally higher in the single-shot SSFP images, it is important to point out that 7/32 subjects had breath-held segmented LGE imaging that was nearly uninterpretable, with a quality score of 1 or 2, because of artifacts from respiratory motion or sinus arrhythmia or cardiac ectopy. When patients had difficulty holding their breath or had significant arrhythmias, the resultant image was typically uninterpretable. These seven individuals had improved ssSSFP quality scores of >3, making a clinical interpretation possible. Figures 3 and 4 demonstrate two such examples, with the accompanying rhythm strip during LGE imaging, located below the images.

Effect of heart rate and heart rhythm on single-shot SSFP score

The subset of eight patients with ectopy or arrhythmia had quality scores of mean +/− SD 2.6+/−1.1, 3.1+/−1.2 and 3.6+/−1.3 for segFLASH, segSSFP and ssSSFP, respectively, although this was not statistically significant, possibly because of the small group size ($P=0.243$ by ANOVA).

We also examined the relationship between R-R interval and quality because the acquisition window for ssSSFP is longer than either of the segmented methods and is more prone to image degradation from cardiac motion. A weak correlation was observed between R-R interval and quality score ($R^2=0.31$) when all 192 data points were included. When broken down into all free-breathing and all segmented breath-held data, the correlation between R-R interval and quality score was $R^2=0.44$ for free-breathing and $R^2=0.34$ for breath-held data, respectively, indicating no significant quality differences in either methodology attributable to heart

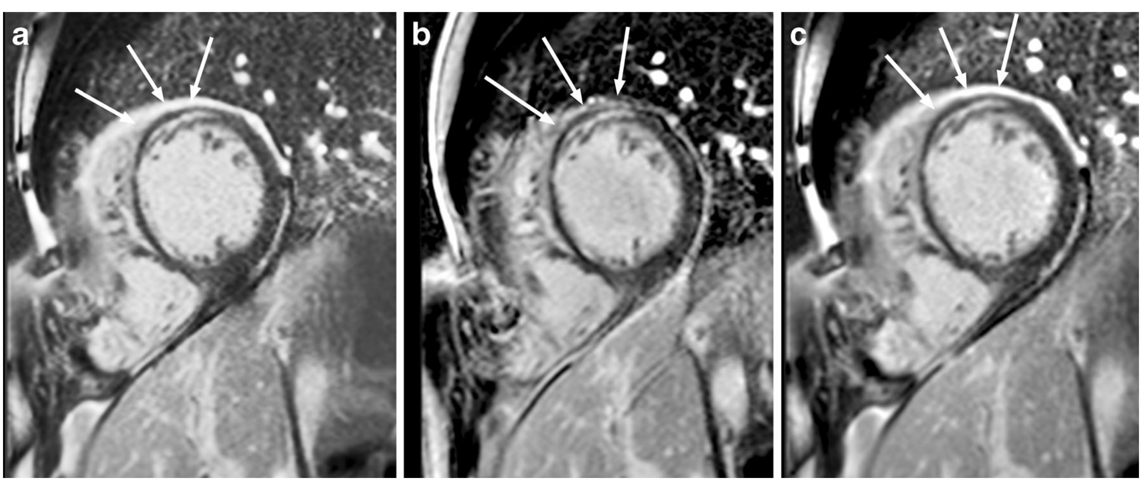

Fig. 2 Late-gadolinium-enhancement imaging imaging using three techniques in an 18-year-old man status post arterial switch operation and with a history of perioperative infarction. **a** Quality score = 5. Segmented SSFP image (FOV 332 × 249, slice thickness 8 mm, flip angle 50°, TR/TE 2.91/1.23 ms, matrix size 256 × 144, 3 shots per slice, 48 views per segment, trigger time 2). **b** Quality score = 4.5. Segmented FLASH image (FOV 332 × 249, slice thickness 8 mm, flip angle 25°, TR/TE 8.31/3.2 ms, matrix size 256 × 144, 6 shots per slice, 24 views per segment, trigger time 2). **c** Quality score = 5. Single-shot SSFP image (FOV 332 × 249, slice thickness 8 mm, flip angle 50°, TR/TE 2.91/1.23 ms, matrix size 256 × 144, parallel imaging with rate 2 acceleration, single shot, trigger time 2). All three images clearly show the late enhancement in the anterior wall of the left ventricle (*arrows*). *FLASH* fast low angle shot, *FOV* field of view, *SSFP* steady-state free precession, *TE* echo time, *TR* repetition time

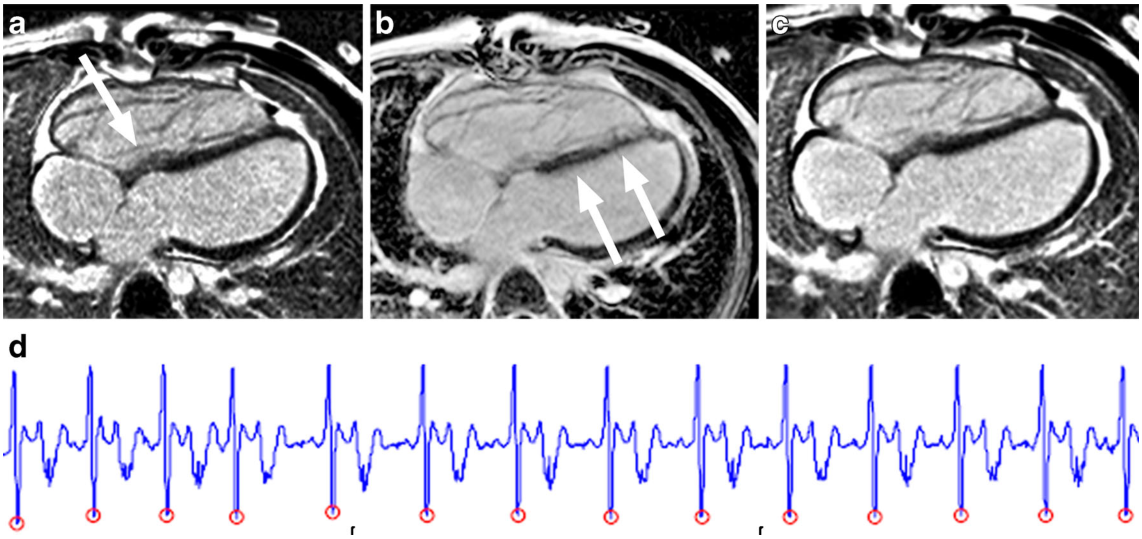

Fig. 3 Late-gadolinium-enhancement imaging using three techniques in a 7-year-old girl. **a** Quality score = 4. Segmented SSFP image (FOV 332 × 249, slice thickness 8 mm, flip angle 50°, TR/TE 2.91/1.23 ms, matrix size 256 × 144, 3 shots per slice, 48 views per segment, trigger time 2). **b** Quality score = 2. Segmented FLASH image (FOV 332 × 249, slice thickness 8 mm, flip angle 25°, TR/TE 8.31/3.2 ms, matrix size 256 × 144, 6 shots per slice, 24 views per segment, trigger time 2). **c** Quality score = 5. Single-shot SSFP image (FOV 332 × 249, slice thickness 8 mm, flip angle 50°, TR/TE 2.91/1.23 ms, matrix size 256 × 144, parallel imaging with rate 2 acceleration, single shot, trigger time 2) in the four-chamber view. Note the cardiac blur from motion of the interventricular septum (*arrows* in **a**, **b**), presumably related to the significant sinus arrhythmia this girl had during the scan. **d** Vectocardiogram tracing during the acquisition. *FLASH* fast low angle shot, *FOV* field of view, *SSFP* steady-state free precession, *TE* echo time, *TR* repetition time

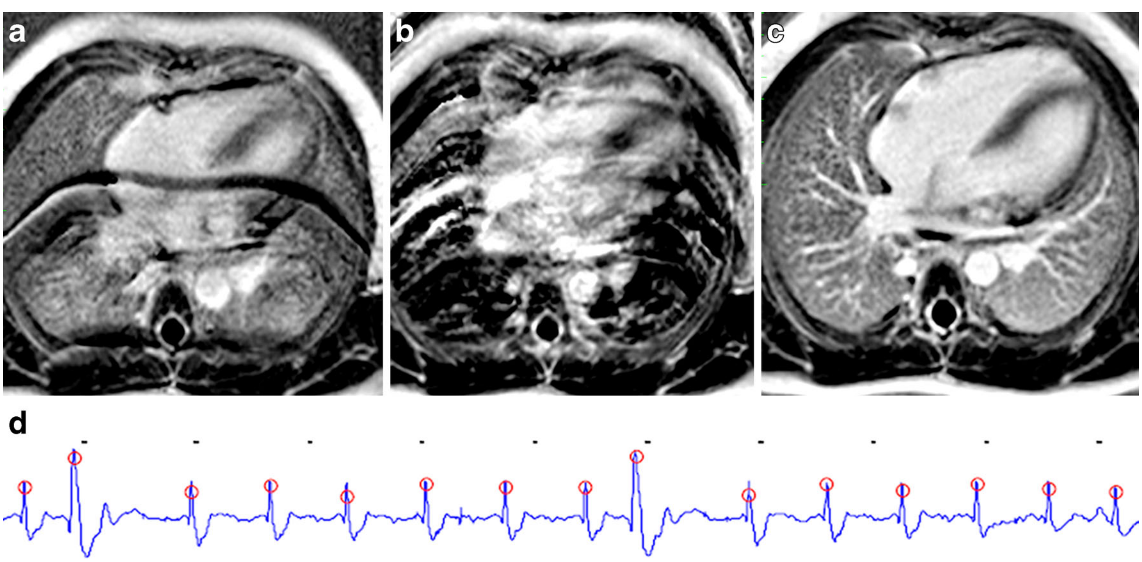

Fig. 4 Late-gadolinium-enhancement imaging using three techniques in a 12-year-old girl with tetralogy of Fallot. **a** Quality score = 2. Segmented SSFP image (FOV 332 × 249, slice thickness 8 mm, flip angle 50°, TR/TE 2.91/1.23 ms, matrix size 256 × 144, 3 shots per slice, 48 views per segment, trigger time 2). **b** Quality score = 1. Segmented FLASH image (FOV 332 × 249, slice thickness 8 mm, flip angle 25°, TR/TE 8.31/3.2 ms, matrix size 256 × 144, 6 shots per slice, 24 views per segment, trigger time 2). **c** Quality score = 4. Single-shot SSFP image (FOV 332 × 249, slice thickness 8 mm, flip angle 50°, TR/TE 2.91/1.23 ms, matrix size 256 × 144, parallel imaging with rate 2 acceleration, single shot, trigger time 2) in the four-chamber view. There is significant motion artifact in (**a**) and (**b**), presumably from the intermittent ventricular ectopy this girl experienced during the scan. The motion artifact is notably absent in (**c**), the free-breathing single-shot technique. **d** Vectocardiogram tracing done during the acquisition that shows premature ventricular contractions. *FLASH* fast low angle shot, *FOV* field of view, *SSFP* steady-state free precession, *TE* echo time, *TR* repetition time

rate. There were fewer low (1 and 2) scores in the free-breathing group, but there was a similar spread of heart rates, which may be why the R2 values for the free-breathing and breath-held groups are both higher than the total R2 value.

Discussion

Late-gadolinium-enhancement techniques in cardiac MR imaging are invaluable in a variety of conditions and therefore it is clinically important to optimize this sequence for children with heart conditions including myocarditis, cardiomyopathy and congenital heart disease. This work introduces a new LGE imaging technique — single-shot free-breathing SSFP (ssSSFP) — and shows that this technique produces images that are equal in quality to segmented approaches. Further, LGE imaging that is normally degraded by arrhythmia, breathing motion and cardiac motion can be improved upon using this technique. Although ideally this work would have compared diagnostic accuracy between ssSSFP and the other techniques, because of the low incidence of LGE in the pediatric population we used image-quality scores instead.

Single-shot SSFP LGE imaging clearly has utility in any patient who cannot perform a breath-hold [14], and this work demonstrates that ssSSFP with respiratory-motion-corrected averaging can be performed with adequate resolution in small children with higher heart rates. This imaging method also has utility in children with an irregular heart rate, including those with significant sinus arrhythmia or atrial/ventricular ectopy, and it performs well in this subset of patients, although a direct comparison with standard arrhythmia rejection methods was outside the scope of this study. Overall, twice as many children had high-quality diagnostic LGE images using the free-breathing motion-corrected imaging strategy when compared to either of the segmented strategies. This translates into decreasing the overall time of studies when repeat imaging is needed, decreasing the number of failed studies where arrhythmia or breathing motion precludes segmented LGE imaging, and decreasing the time of LGE imaging because fewer slices need repeating.

On a more global scale, the single-shot motion-corrected free-breathing technique significantly reduces the need for general anesthesia during LGE imaging and reduces the need for sedation in centers where free-breathing techniques are already used for ventriculography and angiography in children. Generally speaking, the motion correction algorithm has two components: (a) discarding motion-corrupted data and (b) deforming the remaining data to a target image. Both components enable successful averaging of multiple beats. Motion correction allows for registration of images across the respiratory cycle and elimination of motion-degraded imaging. Subsequent averaging of these images creates a higher signal-to-noise ratio, so the overall effect is to deliver an image with high-quality spatial resolution that is robust in the face of respiratory motion, thus eliminating the need to suspend respiration.

The single-shot SSFP LGE technique is limited in children with R-R intervals less than 400 ms given the acquisition time of ~120–220 ms, depending on matrix size. Therefore it may not be appropriate for the smallest infants and those with a heart rate >150 bpm. In these cases, breath-held segmented imaging or averaged segmented imaging may be superior because of its ability to decrease the number of cardiac segments and limit cardiac motion in the image. There may be an interest in developing a respiratory navigator to allow for free-breathing segmented imaging in this cohort. However with the advent of newer receiver coils with smaller elements designed for infant imaging, increased signal-to-noise ratios may be favorable to drive up the parallel imaging factors to a point where it is realistic to obtain single-shot imaging at even higher heart rates. Also, there was not a significant degradation in quality of the free-breathing technique at higher heart rates in this study. The ideal acquisition window length and trigger delay in single-shot late enhancement could be the subject of future study.

This study was limited by the overall incidence of the presence of late gadolinium enhancement, which was only found in four subjects. In children LGE findings are less common than in adults undergoing MRI for ischemic heart disease evaluation. The prevalence of LGE in the studied cohort was similar to that in our general pediatric population. In each of those subjects, LGE was detected with the ssSSFP. There were no studies where LGE was detected on the segmented images and not the single-shot free-breathing images. Another limitation is that it is difficult to be truly blinded to reviewing a FLASH versus an SSFP LGE image, although the images were evaluated without any identifiers or markings. An additional limitation of this study is that it only focused on the left ventricle, which can be imaged in diastole, whereas the right ventricle is optimally imaged in systole, where it is thicker. Finally, because various institutions rely on a systolic acquisition for LGE imaging at higher heart rates, it should be noted that because the single-shot technique employs a long acquisition window, systolic imaging would suffer significantly from blurring. A separate validation study should be conducted to explore feasibility and optimized parameters for the single-shot approach in that context.

Conclusion

Single-shot late-enhancement imaging with motion-corrected averaging in the pediatric population is feasible, robust at high heart rates and with variable R-R intervals, and can be performed without the need for breath-holding and produce higher image-quality ratings than standard breath-held techniques. Use of free-breathing single-shot motion-corrected technique does not compromise LGE image quality in children who can hold their breath, and it can significantly improve image quality in those who cannot hold their breath or who have significant arrhythmia.

Acknowledgments This research was supported in part by the Intramural Research Program of the National Institutes of Health, National Heart, Lung, and Blood Institute, and through NHLBI contract award HHSN268201500001C.

Compliance with ethical standards

Conflicts of interest None

References

1. Babu-Narayan SV, Kilner PJ, Li W et al (2006) Ventricular fibrosis suggested by cardiovascular magnetic resonance in adults with repaired tetralogy of Fallot and its relationship to adverse markers of clinical outcome. Circulation 113:405–413
2. Secinaro A, Ntsinjana H, Tann O et al (2011) Cardiovascular magnetic resonance findings in repaired anomalous left coronary artery to pulmonary artery connection (ALCAPA). J Cardiovasc Magn Reson 13:27
3. Hor KN, Taylor MD, Al-Khalidi HR et al (2013) Prevalence and distribution of late gadolinium enhancement in a large population of patients with Duchenne muscular dystrophy: effect of age and left ventricular systolic function. J Cardiovasc Magn Reson 15:107
4. Chan RH, Maron BJ, Olivotto I et al (2014) Prognostic value of quantitative contrast-enhanced cardiovascular magnetic resonance for the evaluation of sudden death risk in patients with hypertrophic cardiomyopathy. Circulation 130:484–495
5. Mavrogeni S, Bratis K, Georgakopoulos D et al (2012) Evaluation of myocarditis in a pediatric population using cardiovascular magnetic resonance and endomyocardial biopsy. Int J Cardiol 160:192–195
6. Ylänen K, Poutanen T, Savikurki-Heikkilä P et al (2013) Cardiac magnetic resonance imaging in the evaluation of the late effects of anthracyclines among long-term survivors of childhood cancer. J Am Coll Cardiol 61:1539–1547
7. Simonetti OP, Kim RJ, Fieno DS et al (2001) An improved MR imaging technique for the visualization of myocardial infarction. Radiology 218:215–223
8. Rangamani S, Varghese J, Li L et al (2012) Safety of cardiac magnetic resonance and contrast angiography for neonates and small infants: a 10-year single-institution experience. Pediatr Radiol 42: 1339–1346
9. Huber A, Schoenberg SO, Spannagl B et al (2006) Single-shot inversion recovery TrueFISP for assessment of myocardial infarction. AJR Am J Roentgenol 186:627–633
10. Huber A, Bauner K, Wintersperger BJ et al (2006) Phase-sensitive inversion recovery (PSIR) single-shot TrueFISP for assessment of myocardial infarction at 3 tesla. Investig Radiol 41:148–153
11. Kellman P, Larson AC, Hsu L-Y et al (2005) Motion-corrected free-breathing delayed enhancement imaging of myocardial infarction. Magn Reson Med 53:194–200
12. Ledesma-Carbayo MJ, Kellman P, Hsu L-Y et al (2007) Motion corrected free-breathing delayed-enhancement imaging of myocardial infarction using nonrigid registration. J Magn Reson Imaging 26:184–190
13. Kellman P, Arai AE (2012) Cardiac imaging techniques for physicians: late enhancement. J Magn Reson Imaging 36:529–542
14. Piehler KM, Wong TC, Puntil KS et al (2013) Free-breathing, motion-corrected late gadolinium enhancement is robust and extends risk stratification to vulnerable patients. Circ Cardiovasc Imaging 6:423–432
15. Chefd'hotel C, Hermosillo G, Faugeras O (2002) Flows of diffeomorphisms for multimodal image registration. Proc IEEE Int Symp Biomed Imaging, pp 753–756. doi:10.1109/ISBI.2002.1029367
16. Hermosillo G, Chefd'hotel C, Faugeras O (2002) Variational methods for multimodal image matching. Int J Comput Vis 50: 329–343